Pathol. Oncol. Res. (2012) 18:939–947
DOI 10.1007/s12253-012-9524-x

RESEARCH

Mathematical Modeling of Therapeutic Strategies for Myeloid Malignancies

Dan Wu · Huiyu Li · Wen Du · Xiaoxia Ji · Wei Liu · Shiang Huang · Yi Xiao

Published online: 29 July 2012

Abstract The existence of malignant stem cells has been proven for hematopoietic disorder as well as some solid tumors. Although significant improvements in cancer therapy have been made, tumor recurrence is frequent and can partly be due to the absence of therapeutic target which tumor stem cells are regarded as. In this paper we shall explore different therapeutic scenarios for successful tumor treatment by using a predictive mathematical model based on the cell compartment method. In particular, we shall study the effects of the chemotherapeutic target rate and of the interval of G-CSF administration on therapy for myeloid malignancies through simulating chemotherapy with G-CSF (granulocyte colony-stimulating factor) support. The results indicate that if target rate is raised to an enough high value, the efficiency of chemotherapy increases so greatly that the tumor mature cells perish completely and normal mature cells are maintained at a normal level. Furthermore, the administration of G-CSF can increase the amount of the normal mature cells to a normal level. However, too long interval of G-CSF administration is demonstrated not propitious to patients' healing. These results indicate that the simulations may be an effective approach to help designing therapeutic scenarios for successful tumor treatment by chemotherapy.

D. Wu · X. Ji · Y. Xiao (✉)
Department of Physics,
Huazhong University of Science and Technology,
Wuhan, China
e-mail: yxiao@mail.hust.edu.cn

H. Li · W. Du · W. Liu · S. Huang (✉)
Center of Stem cell, Tongji Medical College,
Huazhong University of Science and Technology,
Wuhan, China
e-mail: sa2huang@hotmail.com

Keywords Hematopoietic stem cells · Cancer stem cell · Mathematical modeling · Chemotherapy

Introduction

Stem cells are defined as cells that have the ability to perpetuate themselves through self-renewal and to generate mature cells of a particular tissue through differentiation. Hematopoietic stem cells (HSCs) have been shown to be responsible for the generation and regeneration of the blood-forming and immune (haematolymphoid) systems [1]. Normal cell turnover translates in the production of approximately 10^{12} cells every day [2]. Cellular proliferation harbors the risk of acquiring mutations because the genome replication machinery is not perfect. Serial accumulation of mutations increases the probability of malignant transformation, especially if the mutations occur in long-lived cells [3]. Recently, the existence of these malignant stem cells has been proven for myeloid malignancies as well as some solid tumors. Stem cells display several phenotypic characteristics that are considered critical for the acquisition of the tumor phenotype, including the potential for unlimited cell replication, self-sufficiency and long-term survival [4]. It is thus likely that many hematologic malignancies, such as myeloproliferative disorders and chronic myeloid leukemia (CML), originate from the hematopoietic stem cell compartment [5]. Many signaling pathways associated with normal stem cells are also be involved in regulating the development of cancer cells, for example, Bmi-1[6], Wnt signaling [7], and sonic hedgehog [7], which are all implicated in both oncogenesis and stem cell renewal.

Mathematical modeling and computational approaches can contribute to the understanding of complicated cell mechanisms and tissue physiology. Mathematical modeling

of cancer initiated in the 1950s [8] has led to considerable insight into the disease [9]. Some theories also appeared for cancer treatment and resistance [10].

For the hematopoietic system, there are some proposed physiological and disease models. Some mathematical models were applied to investigate the oscillating phenomena within the hematopoietic system in different patho-physiological disorders [11–13]. Myeloproliferative disorders were investigated, which can be explained by a loss of microenvironmental control of stem cells [14]. Using an ordinary differential equation model of human granulopoiesis, Engel et al. [15] were able to consistently describe the effects of ten different multicycle poly-chemotherapies on leukocyte numbers in lymphoma patients. Ostby et al. [16] proposed another model of human granulopoiesis based on partial differential equations and applied this model successfully to granulocyte reconstitution after high-dose chemotherapy with stem cell and G-CSF support in breast cancer patients.

A mathematical model was proposed for the hematopoietic system based on the cell compartments method, which considers stem cells, erythropoietic and granulopoietic progenitors and precursors, and two essential regulatory functions (self-renewal probability and fraction of stem cells in active cell cycle) [17]. Moreover, the influence of erythropoietin on erythropoietic amplification was also investigated. Based on Wichmann's model, Ganguly et al. studied formation of cancer cells from stem cells [18]. They ascribed the growths of abnormal (stem and progeny) cells from their normal counterparts with separate mutation probabilities and predicted that stem cell mutations are more significant for the development of cancer than a similar mutation in the early progenitor cells.

To quantify the dynamics of bone marrow recovery after the suppressing and stimulating disturbances of cytotoxic drugs, Scholz [19] constructed a biomathematical compartment model of human granulopoiesis under polychemotherapy with G-CSF support, which gave reliable predictions concerning the myelotoxicity of any given chemotherapy regimen based on the cytotoxic drugs considered. Moderate intensification of multicyclic polychemotherapy has been shown to improve the therapeutic results for lymphomas [19]. The chemotherapeutic drugs are applied several times in fixed time intervals so as to obtain a better therapeutic effect. However, Scholz et al. [19] also indicated that a major limit of such intensified regimen is that leucopenia induced by the side effects of cytotoxicity of drugs administered in polychemotherapy. In clinic, the granulopoietic growth actor G-CSF is often applied to reduce the neutropenic period.

Despite significant improvements in cancer therapy, tumor recurrence is frequent due to a variety of mechanisms, including the evolution of resistance and tumor progression. Recent research confirms that many neoplastic diseases like breast cancer [20], prostate cancer [21], liver cancer [22], or leukemia [23], can occur because of mutations in normal stem and/or early progenitor cells. Moreover, it has been shown that various genes regulating the self-renewal in normal cells are also found in cancer cells [24]. It is known that most cancers are not clonal, but consist of heterogeneous sub-populations with distinct characteristics within a single neoplasm. These sub-populations are similar to the hierarchical tree of stem cell lineages. These results manifest the so-called stem cell cancer hypothesis, claiming that some cancers have stem cell origin. However, tumor stem cells were not targeted by standard therapy and might be responsible for treatment failure and tumor recurrence in many patients. In order to quantitatively understand this problem, in this paper we use mathematical model to explore different therapeutic scenarios and illustrate the properties required by novel therapeutic agents for successful myeloid malignancies treatment.

Model

In order to provide a quantitative basis for designing a chemotherapy scenario, we simulate the human hematopoiesis under chemotherapy with G-CSF support by using a mathematical model which was proposed by Wichmann et al., Ganguly et al. and Scholz et al. [18]. Modifications has also been made, such as re-evaluating values of some parameters and applying some new parameters into the model, in order to take account of experimental results and clinical therapy. The modifications include: (i) The ratio of the population of hematopoietic stem cells and that of mature granulocyte after homeostasis is taken as the experimental value $1{:}10^4$ [25], instead of 1:700 [18]; (ii) the division cycle of a hematopoietic stem cell is taken as the experimental value 12 h [25]; (iii) the difference of the self-renewal probabilities between the early progenitor subgroups is taken into account; (iv) In order to simulate the therapeutic method, some new parameters have been applied to the model, including the chemotherapeutic target rate and the production rate from abnormal early progeny. To address the dynamics of normal and abnormal cells more clearly, the model consists of two parts, one of which describes the evolution of normal cell population, and the other of which is for the evolution of abnormal cell population.

The Evolution of Normal Cell Population

The time-dependent evolution of normal cell population of each subtype is described by a system of ordinary differential equations [18]. Some kinetic rates in the model are defined in Tables 1 and 2, and the values of kinetic rates

and other parameters are adapted from the literature based on haematopoietic system.

$$\frac{dN_{SC}}{dt} = \omega_{SC}(2P_{SC} - 1)N_{SC} - \omega_{SC}M_{SC}N_{SC} - (1-\beta)k_{x0}\Psi_{SC}N_{SC} \tag{1}$$

$$\frac{dN_{EP1}}{dt} = 2\omega_{SC}(1 - P_{SC})N_{SC} - \omega_{EP1}N_{EP1} - (1-\beta)k_{x1}\Psi_{CX}N_{EP1} \tag{2}$$

$$\frac{dN_{EPi}}{dt} = \omega_{EPi-1}(2P_{EPi-1} - M_{EP})N_{EPi-1} - \omega_{EPi}N_{EPi} - (1-\beta)k_{x1}\Psi_{CX}N_{EPi}\ i = 2\ldots k \tag{3}$$

$$\frac{dN_{LP}}{dt} = Z_{in}\left(\sum_{i=1}^{k-1} 2\omega_{EPi}(1 - P_{EPi})N_{EPi} + 2\omega_{EPk}N_{EPk}\right) - \omega_{LP}N_{LP} - (1-\beta)k_{x1}\Psi_{CX}N_{LP} \tag{4}$$

$$\frac{dN_{MC}}{dt} = N_{LP}^{out} - \omega_{0,MC}N_{MC} - \frac{(1-\beta)\Psi_{CX}}{T_{nor}(1 + T_{pred}\Psi_{pred})}N_{MC} \tag{5}$$

From Eqs. (1), (2), (3), (4) and (5), N with different subscripts denotes the cell population of each subtype. The subscripts represent stem cell (SC), the ith subcompartment of early progenitor cell (EPi), late progenitor cell (LP) and mature cell (MC) respectively. $\omega = ln2(\alpha/\tau)$ denotes the cell division rate, in which τ is the cell cycle time (Table 1) and α is the mitotic fraction (Table 2). M with subscripts is the mutational probability for different cell subtype. $N_{LP}{}^{out} = 2^5 Z_{out}\omega_{LP}N_{LP}$ is the efflux from the LP compartment i.e. the generation rate of mature cells. Tables 1 and 2 in Appendix give the details of the parameters in equations.

The LP cells undergo n_{LP} successive stages of cell division before transforming into mature cells, where $n_{LP} = n_{LP}(N_{MC}) \in [n_{LP,\min}, n_{LP,\max}]$ (see Table 2). The model follows an approach [17, 18] that assumes that the efflux from the EP compartment to the LP compartment is amplified by a factor Z_{in}. Immediately before leaving the LP compartment, the population of cells is further amplified by a factor Z_{out}, which satisfies $Z_{in} \times Z_{out} = 2^{nLP}$, and the factor $Z_{in} = (2^{nLP}\text{-}1)\tau_g / T_{LP} + 2^{nLP}\tau_m / T_{LP}$. The average generation time for each division can be expressed as $\tau_g = \tau_{LP}/\alpha_{LP}$. So $T_{LP} = n_{LP} \times \tau_g + \tau_m$ can be interpreted as the average transit time through compartment progenitor cells and consists of the proliferating part $n_{LP} \times \tau_g$ and the maturating part τ_m.

The last terms in the right hand side of Eqs. (1), (2), (3), (4) and (5) describe the effect of chemotherapy, which have a form proposed by Scholz et al. [19]. We also introduce a new parameter β to denote the target rate (e.g., β=0.85 means that the 85% of normal cells will not be by influenced by chemotherapy, but the rest 15% will be exposed to chemotherapy). The values of all other parameters used in [19] are applied in this paper. k_{x0} and k_{x1} are toxicity parameters for the drug combinations C750+D50+V2 applied in the BEACOPP regimens and are set as 0.1775 and 0.098 for the younger patients and 0.1951 and 0.5 for the elderly patients respectively [19]. The characteristic chemotherapy function Ψ_{cx} is defined as below [19]:

$$\Psi_{CX}(t) = 1\ if \exists i : t_i < t \le t_i + 24\ else\ \Psi_{CX}(t) = 0 \tag{5a}$$

where $t_i(i=1,\ldots,M)$ is the time points of administration of cytotoxic drugs during chemotherapy and assumes that single application of cytotoxic drugs induces an instantaneous depletion in each cell stage of bone marrow that continues for 24 h.

The effect of steroid prednisone, which is administered as a supportive therapy in chemotherapy, is included in the last term in the right hand side of Eq. (5). In Eq. (5), T_{pred} represents the percentage of prolongation of the transit time and Ψ_{pred} is the characteristic function of prednisone administration. The later is defined in the same form as the characteristic function of chemotherapy, i.e., the prednisone effect keeps also 24 h after administration [19]. $T_{nor}(1 + T_{pred}\Psi_{pred})$ is defined as the average transit time of cells and T_{nor} is the transit time in normal condition.

The Evolution of Abnormal Cell Population

The evolutions of abnormal cell population of each subtype have been given by [18]:

$$\frac{dN_{ASC}}{dt} = \omega_{SC}(2P_{ASC} - 1)N_{ASC} + \omega_{SC}M_{SC}N_{SC} - k_{y0}\Psi_{CX}N_{ASC} \tag{6}$$

$$\frac{dN_{AEP1}}{dt} = 2\omega_{SC}(1 - P_{ASC})N_{ASC} - \omega_{EP1}N_{AEP1} - k_{y1}\Psi_{CX}N_{AEP1} \tag{7}$$

$$\frac{dN_{AEPi}}{dt} = 2\omega_{EPi-1}P_{EPi-1}N_{AEPi-1} - \omega_{EPi}N_{AEPi} + \omega_{EPi-1}N_{EPi-1}M_{EP} - k_{y1}\Psi_{CX}N_{AEPi}\ i = 2\ldots k \tag{8}$$

$$\frac{dN_{AP}}{dt} = \gamma N^{out}{}_{AEP} - \omega_{0,AP}N_{AP} - \frac{\Psi_{CX}}{T_{nor}(1 + T_{pred}\Psi_{pred})}N_{AP} \tag{9}$$

N with different subscripts denotes the cell population of each subtype. The subscripts represent abnormal stem

cell (*ASC*), the *i*th subcompartment of abnormal early progenitor cell (*AEPi*), and abnormal progeny compartment (*AP*) respectively. k_{y0} and k_{y1} are toxicity parameters and are set as the same value as k_{x0} and k_{x1}. $N_{AEP}{}^{out} = 2^5 Z_{in}(\sum_{i=1}^{k-1} 2\omega_{EPi}(1-P_{EPi})N_{AEPi} + 2\omega_{EPk}N_{AEPk})$ denotes the overall outflux of abnormal *EP* cells. Different from the previous model [18], the efflux from the abnormal early progenitors is amplified by a factor Z_{in}. One reason is the proliferation of cancer stem cells and abnormal early progenitors are more uncontrolled than that of normal ones. The other reason is the efflux from the normal early progenitors is amplified by a factor Z_{in} (see Eq. (4)). Furthermore, to explore the therapeutic method better, a new parameter γ is introduced to denote the production rate from abnormal *EP* cells.

The values of all the parameters are listed in Table 1 of Appendix [26] unless stated in some figures. The 4th order Runge–Kutta algorithm has been applied to integrate Eqs. (1), (2), (3), (4), (5), (6), (7), (8) and (9) with a time step of 0.001 h to simulate the behavior of the model. In all the calculations, an initial normalized condition N_{SC}=1 is selected, with all other normalized cell populations being set to zero.

Results

The Evolution of Cell Population without Chemotherapy

Since some modifications to the parameters used in [17, 18] have been made in the paper, we will validate the model represented by Eqs. (1), (2), (3), (4), (5), (6), (7), (8) and (9). We first simulate the model behaviors without considering chemotherapy in Figs. 1 and 2, i.e., Ψ_{CX}=0. Figure 1 is for normal hematopoiesis, i.e., the cell mutation probabilities M_{SC} and M_{EP} are assumed to be zero. It is shown that the *SC* population reaches a stable value (≈0.87) quickly. After 500 ~600 h, the *LP* and *MC* cell populations also reach steady values of 140 and 13000 respectively. The ratio of N_{SC} and N_{MC} is consistent with the experiment which was performed for human bone marrow stem cells [25]. This confirms that the modeled process is in homeostasis and self-regulative, that is, proper cell signaling regulates cell proliferation to a relatively steady value that is sufficient to replenish the steady death (apoptosis) of mature cells.

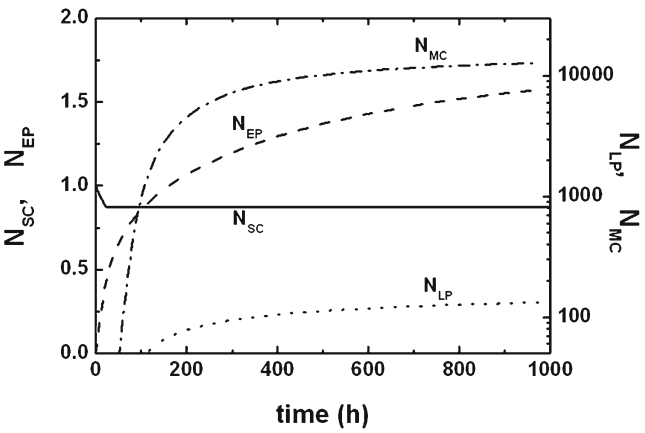

Fig. 1 Numerical simulation of normal hematopoiesis. M_{SC}=M_{EP}=0. N_{SC} (*solid line*) and N_{EP} (*dashed line*) use left y axis; N_{LP} (*dotted line*) and N_{MC} (*dash dotted line*) use right y axis

Figure 2 shows the evolution of *SC*, *ASC*, *MC* and *AP* populations with the occurrence of an oncogenic event either in the *SC* or in the *EP* populations. When the cell mutation occurs only during stem cell self-renewal (with the mutational probability M_{SC} of 0.02) (Fig. 2a and b), the abnormal progeny population grows quickly and suppresses the growth of normal mature cells ultimately, which successfully simulated the loss of self-regulation. However, if only *EP* cells undergo mutation (with the mutational probability M_{EP} set as 0.1, Fig. 2c and d), the *AP* population increases to a stable and relative low level. It implies that, even though there is a group of *AP* compartment, the tumor mature cells will be very easy to be eliminated. With respect to the selection of mutational probability, a range of values of M_{SC} and M_{EP} are picked up to test the evolution of cells compartment(data not shown), which demonstrates that varying the magnitude of different mutational probabilities up to 10-fold will not qualitatively alter the fundamental behaviors of cells evolution. Considering that the recurrence of tumor is frequent in clinic, the model reconfirms the conclusion of the previous studies that there is a much greater opportunity for mutations to accumulate in stem cells than in other cell types [27]. On the other hand, these consistent simulation results indicate that the model and parameters used in this paper are reasonable.

The Evolution of Cell Population with Therapy

In this subsection we focus on the therapy scenario for hematopoietic disorder. As shown in Fig. 2a and b, in the absence of therapy, the tumor takes over and would ultimately drive the normal blood system to extinction. Cancer therapy can affect both the mature cell compartment and the stem cell compartment. The therapeutic effects include increasing the death rate of tumor stem cells, decreasing their proliferation rate, reducing the production rate of differentiated tumor cells, and restoring sensitivity to environment, etc.

The effects of therapy target at mature tumor cells are shown in Fig. 3. In Fig. 3a and b, the death rate of *AP* population $\omega_{0,AP}$ is raised from 0.01 per day to 0.05 per day after 3000 h. Therapy that only increases apoptosis in the mature tumor cells leads to an initial decrease in the tumor

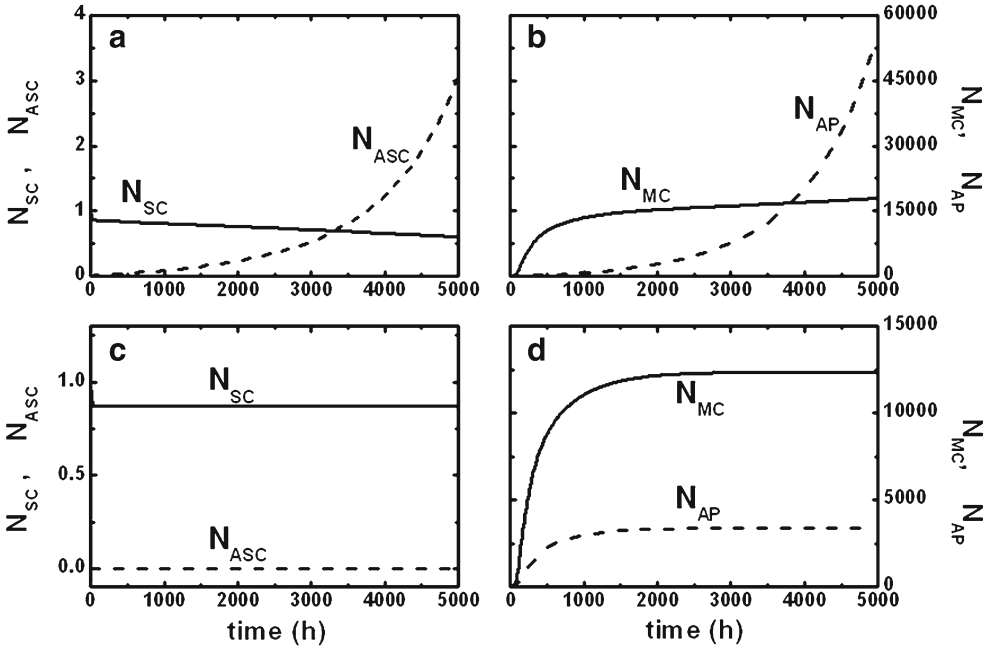

Fig. 2 Numerical simulation of abnormal hematopoiesis. **a** and **b**: M_{SC}=0.02, M_{EP}=0. **c** and **d**: M_{SC}=0, M_{EP}=0.1

burden. However, the pool of tumor stem cell continues to expand (Fig. 3a), so therapy will ultimately fail due to the continuous amplification that occurs in the bone marrow. Similarly, a therapeutic agent that decreases the production rate of mature tumor cells (e.g., imatinib) cannot cure the disorder for the same reason (Fig. 3c and d). It is known that the self-renewal ability in cancer stem cells (CSCs) is poorly controlled, which leads to an abnormal differentiation and a faster proliferation in cancer tissue [28]. Hence, it appears likely that CSCs are often responsible for cancer recurrences after treatment. Therefore, any treatments designed to eradicate the tumor should target the tumor stem cells.

A therapeutic agent designed to selectively inhibit the replication of tumor stem cells can in principle lead to tumor eradication. For example, tumor stem cell proliferation is greatly inhibited (P_{ASC}=0.02) from 3000 h (Fig. 4), the pool of tumor stem cell increases no longer. However, because of the presence of tumor stem cells, the mature tumor cells continue to expand from 3000 h, and begin to decay from about 3500 h (Fig. 4b).

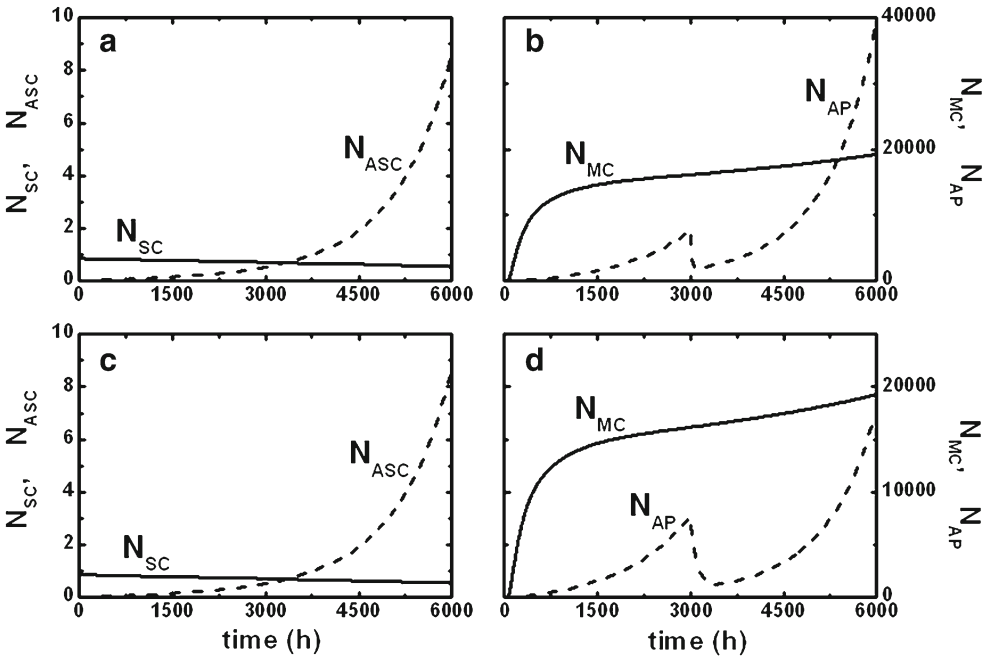

Fig. 3 Therapy target at the differentiated tumor cells. M_{SC}=0.02, M_{EP}=0. **a** and **b** The death rate of differentiated tumor cells $\omega_{0,AP}$ is increased from 0.01 (**a**) to 0.05 (**b**) after 3000 h. **c** and **d** The production rate of differentiated tumor cells γ is decreased from 1.0 (**c**) to 0.1 (**d**) after 3000 h

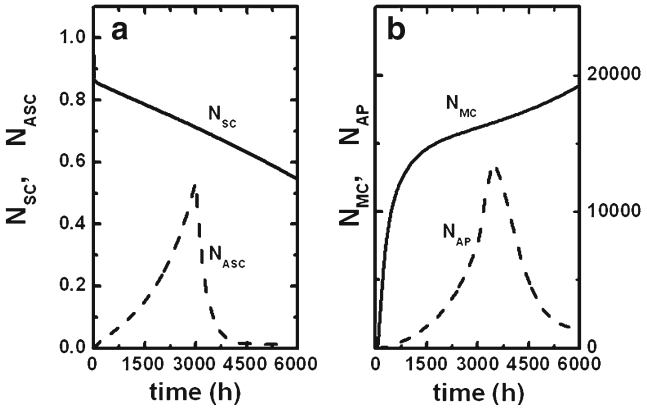

Fig. 4 Therapy target at the tumor stem cells. M_{SC}=0.02, M_{EP}=0. The self-renewal probability of tumor stem cells P_{ASC} is decreased to 0.02 after 3000 h

The Evolution of Cell Population with Chemotherapy

To measure the therapeutic effects of chemotherapy with G-CSF support, Eq. (5a) has been applied in the following simulations. From Fig. 5a to c, the chemotherapy for younger patients starts form 3000 h, and is administrated every 7 days. The tumor cells are eliminated very quickly after applying chemotherapy, but the normal mature cells decay at the same time (Fig. 5a). However, if the target rate of chemotherapy is larger than 0.7, the population of the normal mature cells will not decay greatly and will maintain at a steady level (Fig. 5b). This result shows that, if the target rate is raised to an enough high level, the efficiency of chemotherapy increases so greatly that the cancerous mature cells perish completely and the population of normal mature cells is maintained at a normal level. Furthermore, Fig. 5c demonstrates the relationship between the decay velocities of cells and the target rate of chemotherapy, from which it can be seen that the decay velocities of *MC* and *AP* cells declines with the target rate of chemotherapy decreasing but not in a simple linear relation. This is because abnormal cell compartments that derive from the normal stem cells will be influenced by the later. If the target rate is lower than 0.7, the normal cell compartments decay as quickly as abnormal cell compartments. If the target rate lies in a moderate value, the normal cell population oscillates with each administration of chemotherapy, and both normal mature cells and abnormal cells decay slowly. If the target rate is close to one, the *AP* population decreases almost monotonically. In short, this nonlinear change is induced by the complex relationship between the normal and abnormal compartments, which could give some clues to improve chemotherapeutic effects.

In the chemotherapy for elderly patients (with toxicity parameters for the elderly patients), the normal and abnormal populations decay more quickly than those in younger patients (Fig. 5d). This is because in clinic elderly patients have less tolerance during chemotherapy than younger patients.

As shown in Fig. 5, for target rate under 0.7, both the abnormal cells and the normal cells have been destroyed. So the continued therapy should raise the normal cells to a normal level. In clinic G-CSF (granulocyte colony-stimulating factor) treatment is a general method to stimulate the growth of cells. Mimicking the effects of G-CSF treatment involves modification of four parameters: (1) G-

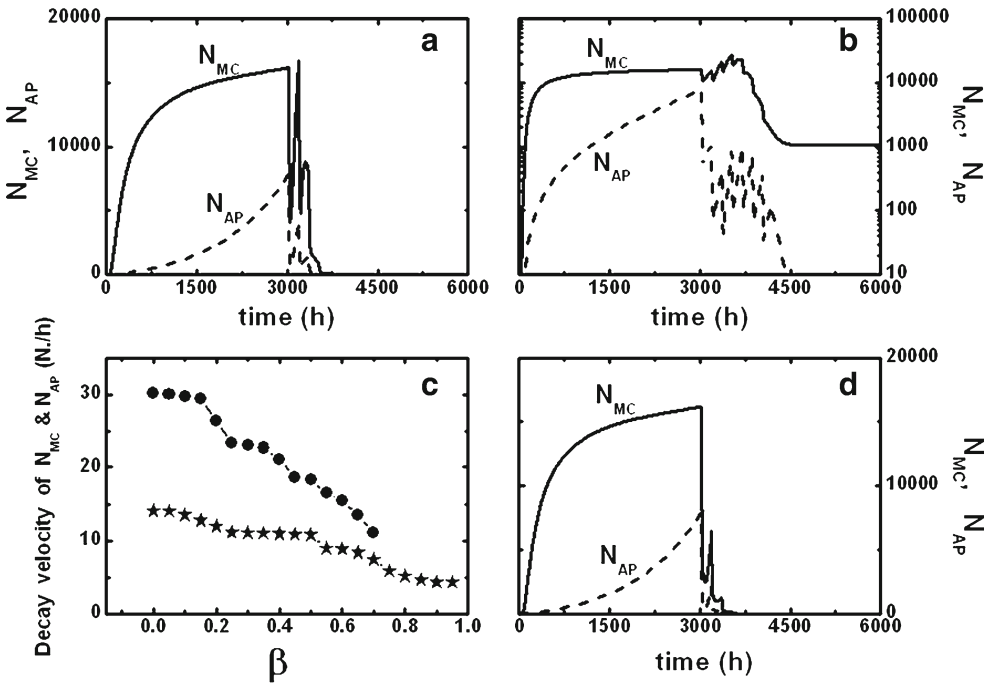

Fig. 5 Chemotherapy. M_{SC}=0.02, M_{EP}=0. Chemotherapy starts after 3000 h, and the interval of chemotherapy is 168 h (7 days). **a** and **b** Chemotherapy for younger patients with the target rate β set as 0.5 (**a**) and 0.85 (**b**) respectively. **c** The decay velocity of abnormal progeny cells (unit is cell number/hour) vs. the target rate of chemotherapy. Circle for N_{MC}, and Star for N_{AP}. **d** Chemotherapy for elder patients. The target rate β is 0.5

CSF decreases the HSC proliferative phase duration τ_{SC} as well as the transit time of neutrophil precursors τ_{EP}; (2) it increases the proliferation rate of normal stem cells P_{SC}; (3) G-CSF was shown to decrease the apoptosis in normal mature cells $\omega_{0,\ MC}$. Bernard et al. [11] showed that the effects of G-CSF could be reproduced by their model (for cyclical neutropenia) if considering these changes in their model parameters.

The effects of every administration will be maintained for 24 h, which includes τ_{SC}=8 h, τ_{EP}=10 h, P_0=0.3 and $\omega_{0,\ MC}$= 0.001. Administration of G-CSF has been applied after 6000 h. When the administration of G-CSF is applied every 24 h (Fig. 6a), the population of normal mature cells expands nearly linearly till reach a normal level. However, if the interval of G-CSF administration becomes longer, the renewal time of normal mature cells becomes longer too, and the steady population of normal mature cells becomes smaller (Fig. 6b). These results imply that too long interval of G-CSF administration is not propitious to patients' healing. The relationship between the renewal time of normal mature cells and the interval of G-CSF administration is given in Fig. 6c. It is easy to understand that the renewal time of normal mature cells increases with the interval of G-CSF administration.

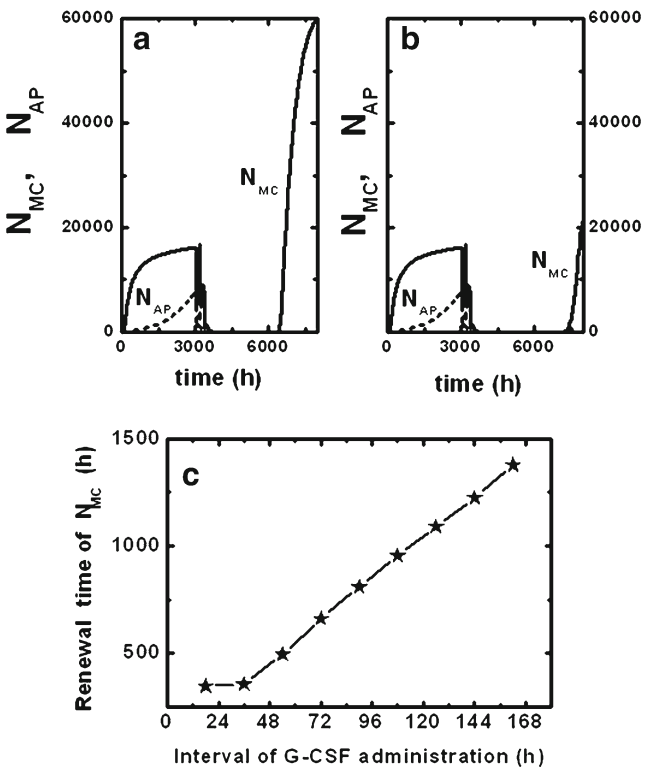

Fig. 6 Chemotherapy with G-CSF support. M_{SC}=0.02, M_{EP}=0. The condition of chemotherapy is the same as in Fig. 5. The target rate β is 0.5. Administration of G-CSF has been applied from 6000 h. The interval of G-CSF administration is (**a**) 24 h, (**b**) 96 h. (**c**) The renewal time of normal mature cells depends on the interval of G-CSF administration

Conclusions

A therapeutic agent designed to inhibit the replication of tumor stem cells can in principle lead to tumor eradication. For a better treatment effect in clinic, the application of chemotherapeutic drugs is repeated several times in fixed time intervals. On the other hand, the granulopoietic growth factor G-CSF is often used to avoid the side effects of chemotherapy. To provide a quantitative basis for these objectives, in this paper a mathematical model is applied to simulate human hematopoiesis under chemotherapy with G-CSF support.

In the simulation for normal circumstances, the model converges to a steady population of the stem cell, early and late progenitor cells, which induce a constant mature cell population. The simulation also shows that, although mutations in stem cells or in EP cells eventually produce the abnormal progeny, mutations in stem cells (rather than in EP cells) lead to uncontrolled growth of the abnormal progeny. The simulation for chemotherapy indicate that the tumor cells are eliminated very quickly after applying chemotherapy, but normal mature cells also decay for most cases. However, if target rate is raised to an enough high value, the efficiency of chemotherapy increases so greatly that tumor mature cells perish completely and normal mature cells are maintained at a normal level. Furthermore, when the administration of G-CSF is applied, the amount of normal mature cells increases nearly linearly to a normal level. However, too long interval of G-CSF administration makes the recovering of the population of *MC* recover much slower, and the steady population of normal mature cells becomes smaller, which implies that too long interval of G-CSF administration is not propitious to patients' healing.

These modeling results indicate that the computer simulations may be an effective approach to help designing therapeutic scenarios for successful tumor treatment by chemotherapy. Specifically, the model could be used as a tool for untested dosing or timing schedules to predict the chemotherapeutic effects and optimize the administration of G-CSF. However, the model of G-CSF applied in this paper is still simple, which doesn't consider the different pharmacokinetics of novel derivates of G-CSF. Moreover, the instantaneous depletion of cell stage influenced by chemotherapy is a rather simplification. Therefore it is useful to address these issues in our future work to provide optimal treatment. On the other hand, chemotherapy has been proven to be very beneficial for many malignancies, the main limit of this therapy is toxicity produced by cytotoxic drugs. So the toxic metabolites following therapy have been taken into attention on experiments and modeling [15], which will be further considered in our future research.

Acknowledgement This work was supported by the National Natural Science Foundation of China under Grant No.30970558 and No.11074084.

Appendix

Table 1 Description of parameters used in the model

Parameters	Symbols	Values	Sources
Cell cycle time for SC compartment	τ_{SC}	12 h	[25, 29, 30]
Cell cycle time for EP compartment	τ_{EP}	14 h	Modification based on [25, 29, 30]
Cell cycle time for LP compartment	τ_{LP}	16 h	Modification based on [25, 29, 30]
Cell maturation time for MC compartment	τ_m	40 h	[17, 18]
Number of EP cell self-renewals	k	5	[17, 18]
Self-renewal probability for EP_1, EP_2, EP_3, EP_4	P_{EP1}, P_{EP2}, P_{EP3}, P_{EP4}	0.5, 0.3, 0.2, 0.1	Modification based on [17, 18]
Upper and lower limits of the number of mitotic cycles	$n_{LP,max}$, $n_{LP,min}$, $n_{LP,norm,}$	9, 3, 4	[17, 18]
Death rate of MC	$\omega_{0,MC}$	0.01	[17, 18]
Death rate of AP	$\omega_{0,AP}$	0.01	[17, 18]
Production rate of AP	γ	1 (if no additional note)	

Table 2 Mathematical representations of the regulatory signals [17, 18]

Controlled parameter	Controlling parameter	Functional relationship
P_{SC}	$N_{SC,}$ $N_{EP,}$ $N_{LP,}$ N_{MC}	$P_{SC} = P_0 \tanh(-Y) + 0.4, where$ $Y = \{(N_{SC} - 1)\max(c_1, \frac{c_1}{N_{SC}^{0.6}}) + \frac{1}{3}c_2(N_{EP} + N_{LP} + N_{MC} - 3)\}$ and $P_0 = 0.1, c_1 = 2, c_2 = -8$
$P_{SC,A}$	$N_{SC,A}$,$N_{EP,A,}$ $N_{LP,A,}$ N_{AP}	$P_{SC,A} = P_{0,A}\tanh(-Y) + 0.4, where$ $Y = \{(N_{SC,A} - 1)\max(c_1, \frac{c_1}{N_{SC,A}^{0.6}}) + \frac{1}{2}c_2(N_{EP,A} + N_{AP} - 2)\}$ and $P_{0,A} = 0.2$
n_{LP}	N_{MC}	$n_{LP} = \frac{1}{\ln 2}\ln\{Z_{max} - (Z_{max} - Z_{min})\exp[-\ln(\frac{Z_{max} - Z_{min}}{Z_{max} - Z_{norm}})N_{MC}^{d}]\}$ where $Z_{max} = 2^{n_{LP,max}}, Z_{min} = 2^{n_{LP,min}}, Z_{norm} = 2^{n_{LP,norm}}, d = 0.84$
$\alpha_{SC,}$ α_{EPi}	$N_{SC,}$ $N_{EP,}$ $N_{LP,}$ N_{MC}	$\alpha = \frac{a_1\exp(-X') + a_2\exp(X')}{\exp(-X') + \exp(X')}$ where $X' = a_3(XS + XE) + a_4$ $XS = bs\begin{cases} In(N_{SC}) & for\ N_{SC} \le 1 \\ (N_{SC} - 1) & for\ N_{SC} > 1 \end{cases}$ and $XE = b_E In\{\frac{1}{3}(N_{EP} + N_{LP} + N_{MC})\}$

b_S=1.0, b_E=0.1. For SC cells, a_1=1.0, a_2=0.01, a_3=1.106, a_4=0.867; For EP_1 cells, a_1=1.0 a_2=0.01, a_3=0.489, a_4=1.553; For EP_2~EP_5 cells, a_1=1.0, a_2=0.3, a_3=0.489, a_4=1.553

References

1. Reya T, Morrison SJ, Clarke MF, Weissman IL (2001) Stem cells, cancer, and cancer stem cells. Nature 414:105–111
2. Abkowitz JL, Persik MT, Shelton GH, Ott RL, Kiklevich JV, Catlin SN, Guttorp P (1995) Behavior of hematopoietic stem cells in a large animal. Proc Natl Acad Sci U S A 92:2031–2035
3. Nowak MA, Michor F, Iwasa Y (2003) The linear process of somatic evolution. Proc Natl Acad Sci U S A 100:14966–14969
4. Hanahan D, Weinberg RA (2000) The hallmarks of cancer. Cell 100:57–70
5. Hope KJ, Jin L, Dick JE (2004) Acute myeloid leukemia originates from a hierarchy of leukemic stem cell classes that differ in self-renewal capacity. Nat Immunol 5:738–743
6. Molofsky AV, Pardal R, Iwashita T, Park IK, Clarke MF, Morrison SJ (2003) Bmi-1 dependence distinguishes neural stem cell self-renewal from progenitor proliferation. Nature 425:962–967
7. Polakis P (2000) Wnt signaling and cancer. Genes Dev 14:1837–1851
8. Armitage P, Doll R (1954) The age distribution of cancer and a multi-stage theory of carcinogenesis. Br J Cancer 8:1–12
9. Michor F, Hughes TP, Iwasa Y, Branford S, Shah NP, Sawyers CL, Nowak MA (2005) Dynamics of chronic myeloid leukaemia. Nature 435:1267–1270
10. Komarova NL, Wodarz D (2005) Drug resistance in cancer: principles of emergence and prevention. Proc Natl Acad Sci U S A 102:9714–9719
11. Bernard S, Belair J, Mackey MC (2004) Bifurcations in a white-blood-cell production model. C R Biol 327:201–210
12. Pujo-Menjouet L, Mackey MC (2004) Contribution to the study of periodic chronic myelogenous leukemia. C R Biol 327:235–244
13. Colijn C, Mackey MC (2005) A mathematical model of hematopoiesis—I. Periodic chronic myelogenous leukemia. J Theor Biol 237:117–132
14. Catlin SN, Guttorp P, Abkowitz JL (2005) The kinetics of clonal dominance in myeloproliferative disorders. Blood 106:2688–2692
15. Engel C, Scholz M, Loeffler M (2004) A computational model of human granulopoiesis to simulate the hematotoxic effects of multicycle polychemotherapy. Blood 104:2323–2331
16. Ostby I, Kvalheim G, Rusten LS, Grottum P (2004) Mathematical modeling of granulocyte reconstitution after high-dose chemotherapy with stem cell support: effect of post-transplant G-CSF treatment. J Theor Biol 231:69–83
17. Wichmann HE, Loeffler M (1985) Mathematical modeling of cell proliferation: stem cell regulation in hemopoiesis. CRC Press, Boca Raton, Fla
18. Ganguly R, Puri IK (2006) Mathematical model for the cancer stem cell hypothesis. Cell Prolif 39:3–14
19. Scholz M, Engel C, Loeffler M (2005) Modelling human granulopoiesis under poly-chemotherapy with G-CSF support. J Math Biol 50:397–439
20. Dontu G, Al-Hajj M, Abdallah WA, Clarke MF, Wicha MS (2003) Stem cells in normal breast development and breast cancer. Cell Proliferation 36:59–72
21. Brown MD, Gilmore PE, Hart CA, Samuel JD, Ramani VA, George NJ, Clarke NW (2007) Characterization of benign and malignant prostate epithelial Hoechst 33342 side populations. Prostate 67:1384–1396
22. Alison MR (2005) Liver stem cells: implications for hepatocarcinogenesis. Stem Cell Rev 1:253–260
23. Warner JK, Wang JC, Hope KJ, Jin L, Dick JE (2004) Concepts of human leukemic development. Oncogene 23:7164–7177
24. Clarke MF (2004) Neurobiology: At the root of brain cancer. Nature 432:281–282
25. Huang S, Terstappen LW (1994) Formation of haematopoietic microenvironment and haematopoietic stem cells from single human bone marrow stem cells. Nature 368:664
26. Armitage P, Doll R (1957) A two-stage theory of carcinogenesis in relation to the age distribution of human cancer. Br J Cancer 11:161–169
27. Michor F, Iwasa Y, Nowak MA (2004) Dynamics of cancer progression. Nat Rev Cancer 4:197–205
28. Dick JE (2003) Breast cancer stem cells revealed. Proc Natl Acad Sci U S A 100:3547–3549
29. Huang S, Terstappen LW (1992) Formation of haematopoietic microenvironment and haematopoietic stem cells from single human bone marrow stem cells. Nature 360:745–749
30. Huang S, Law P, Francis K, Palsson BO, Ho AD (1999) Symmetry of initial cell divisions among primitive hematopoietic progenitors is independent of ontogenic age and regulatory molecules. Blood 94:2595–2604